

Detachment monitoring of repair mortar applied to historical masonry stone by acoustic emission technique

Alessandro Grazzini¹, Giuseppe Lacidogna², Silvio Valente³ and Federico Accornero⁴

Abstract. In the repair of historical masonry walls, the plaster de-bonding frequently happens because of the long-term mechanical incompatibility of new mortar. A new laboratory methodology is described for evaluate the mechanical adhesion of the repair mortar applied in the restoration work at the Sacro Monte di Varallo (UNESCO heritage site). The acoustic emission (AE) technique has allowed to predict the fracture mode and to evaluate the repair mortar applied to historical masonry stone. This non-destructive methodology was able to identify defects and damages in masonry structures. Through shear tests, the specific geometry of assembled specimen can verify the detachment process of repair mortar. The AE technique permits to estimate the amount of energy released in de-bonding surface between repair mortar and stone during damage process. The authors have elaborated a numerical simulation to follow the experimental data. The evolution of de-bonding process of a plaster in a stone brick – mortar system was assess by means of the Acoustic Emission technique, which can follow the numerical model. Therefore, the experimental procedure was able to characterize the mechanical behavior of detachment mortar, useful for selection of repair plaster applied to historical masonry stone.

Keywords: historical masonry structures, Acoustic Emission, plaster detachment, durability, repair mortar.

1. Introduction

The historical masonry walls need restoration of their original plasters, often damaged by external climatic conditions and in particular by capillary or rain infiltration. However, the mechanical and thermo-hygrometric characteristics of the new dehumidified repair mortars are not compatible with those of historical masonry surface. Often the long-term detachment of repair plasters applied to historical masonry walls determines the failure of the restoration work. A preliminary study was need in order to test the compatibility of repair mortars in relation to the great variety of construction techniques with which the historical walls were made. The choice

¹ Assistant Professor (corresponding author), Department of Structural, Geotechnical and Building Engineering, Politecnico di Torino, Turin, Italy, alessandro.grazzini@polito.it

² Associate Professor, Department of Structural, Geotechnical and Building Engineering, Politecnico di Torino, Turin, Italy, giuseppe.lacidogna@polito.it

³ Full Professor, Department of Structural, Geotechnical and Building Engineering, Politecnico di Torino, Turin, Italy, silvio.valente@polito.it

⁴ Research Assistant, Department of Structural, Geotechnical and Building Engineering, Politecnico di Torino, Turin, Italy, federico.accornero@polito.it

of mortars with mechanical and thermo-hygrometric characteristics similar to the historical masonries is advisable. In this way, it is possible to guarantee the durability of repair works and to safeguard historical buildings [1-3].

A new experimental procedure, developed at the Non-Destructive Testing Laboratory of the Politecnico di Torino, was tested on specific mixed stone block-mortar specimens. The goal was to assess the mechanical adhesion of the new de-humidified mortars to the historical masonry walls, in order to select in laboratory the best repair material with respect to the durability of the restoration work [4]. The experimental methodology was tested near the “Sacro Monte di Varallo” (UNESCO heritage site in Piedmont - Italy). The “Sacro Monte” is an artistic-religious complex, built between the 15th and 18th centuries, which contains 45 chapels with frescoes and sculptures (see Fig. 1). The chapels were built by means of stone or brick walls, with wooden roofs [2, 3].



Figure 1. Chapel of Christ at Ann's court

Fig. 1 shows the main problem of deterioration on historical façades due to the rising capillary damp and the freezing-thawing cycles. The original plasters risk the detachment due to the cyclic action of the abundant rain. The Acoustic Emission monitoring technique, employed during static shear test, allowed assessing damage evolution and classification [5]. This experimental research analyzed the detachment of historical plasters without frescoes: in this case, it is possible to replace a new lime mortar dehumidified plaster [2, 3].

2. Laboratory tests

Four specimens were assembled by joining stone blocks (similar to those of the Sacro Monte masonry) to symmetrical layers of repair mortar on the two shorter vertical sides of each stone block (Fig. 2). The static test of this particular specimen, monitored by means of the AE technique, was able to assess the adherence behavior between the dehumidified mortar and the masonry structure [4]. The stone surfaces were treated by means of a

pneumatic drill in order to improve the adherence between mortar and stone. The pre-blended natural hydraulic lime mortar is a transpiring material suitable for the restoration of historical masonry damaged by rising capillary action. Young's modulus of this repair mortar was 7000 MPa, the compressive strength, evaluated according to UNI 6556, was 33.8MPa [2].

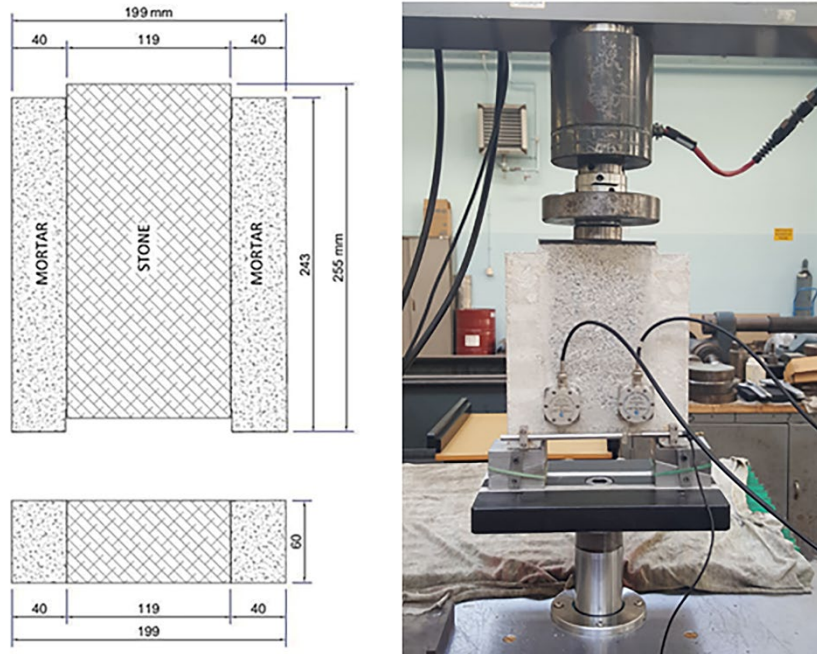


Figure 2. Geometry of mixed specimen

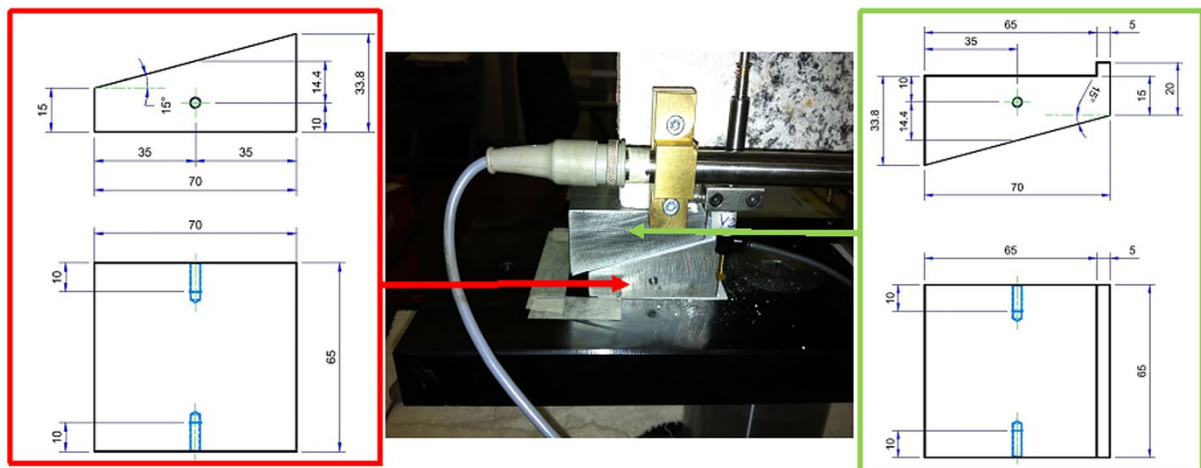


Figure 3. The geometry of the wedges

The dehumidifying mortar layers were applied by a symmetrical discontinuity at the bottom and the top of the specimen (Fig. 2). These notches are useful to trigger the detachment process and assess the adherence capacity of each dehumidified mortar applied to a specific masonry wall. The specimens were instrumented with an inductive horizontal displacement transducer, as shown in Fig. 2. The vertical displacements were recorded by the piston's stroke of the test machine. The shear tests were carried out through monotonous compression load

by controlling the horizontal opening. The mortar layers rested on a double system of steel wedges, as showed in Fig. 3. The steel wedges were coupled by a Teflon layer thick 1 mm in order to for reduce the horizontal friction. The specimens were labeled with “SM” (stone block-mortar), followed by a number indicating the order [1, 2].

3. Monitoring by AE technique

The estimation of active cracks is of significant importance for any structural inspection. For an early warning of crack, the classification of active cracks is a great deal of the AE technique, and in general for Non-destructive monitoring techniques [6]. AE signals due to microcracks were detected by AE sensors attached on the specimen's surface. The signal waveforms were recorded by the AE measurement system. In order to classify active cracks, AE parameters such as rise time and peak amplitude of each signal were considered to calculate the rise angle (RA) value, defined as the ratio of the rise time (expressed in ms) to the peak amplitude (expressed in V). The shape of the AE waveforms is typical of the fracture mode. Shear events are characterized by long rise times and usually high amplitudes, whereas low rise time values are typical of tensile crack propagations. These conditions are synthesized by the RA value [6].

Another parameter used to characterize the cracking mode is the Average Frequency (AF) expressed in kHz. The AF values were obtained from the AE ringdown count divided by the duration time of the signal. The AE ringdown count corresponds to the number of threshold crossings within the duration time. In general, the shift from higher to lower values of AF could indicate the shift of the cracking mode from tensile to shear [6]. Nevertheless, when a cracking process involves the opening of large cracks (Mode I), the frequency attenuation must be a function of this discontinuity. In other words, in this case the wavelength of the AE signals needs to be larger for the crack opening to be overcome, and the shift of the frequencies from higher to lower values could support also a dominant tensile cracking mode.

As regards the AE monitoring, the AE waves, captured by the sensors, were amplified with 60 dB gain before they have been processed, setting the acquisition threshold level up to 2 mV. The AE sensors were attached to the surface of the specimens with a silicon glue, to guarantee a good contact between the sensor and the specimen, also during the final stages of the test.

Briefly, the AE results were shown only for specimen SM4. The load vs. time diagram of the specimen SM4, together with AE cumulated curve and AE rate, is shown in Fig. 4(a-b-c). During the first part of the shear test, the load increases proportionally over time and few AE signals were recorded. However, an increase of the AE signals appeared during each sharply decrease of the load vs. time curve. In fact, the AE signals are related with the energy released in adherence surface during the de-bonding of the mortar (snap-back instabilities) [7].

The linear regression of the signal frequencies (AF) and the signals rise angles (RA) were traced (Fig. 4d-e). Considerable variations from the mean trend were observed in correspondence of specific phases during the test. In the first phase rise angles shows low values, while the frequencies have the higher values more distant from the average trend. This situation is associated to a prevalent tensile crack (Mode I) in the de-bonding

process. In the second phase, the highest values of the RAs were recorded, while the frequencies continue to oscillate with the lowest values. This behavior shows how the delamination process shifts from tensile to shear crack mode, characterized by the sliding of the mortar with respect to the stone block (Mode II). In the final phase not RAs or AF prevails, so there is no prevailing fracture mode before the specimen collapses definitively [1].

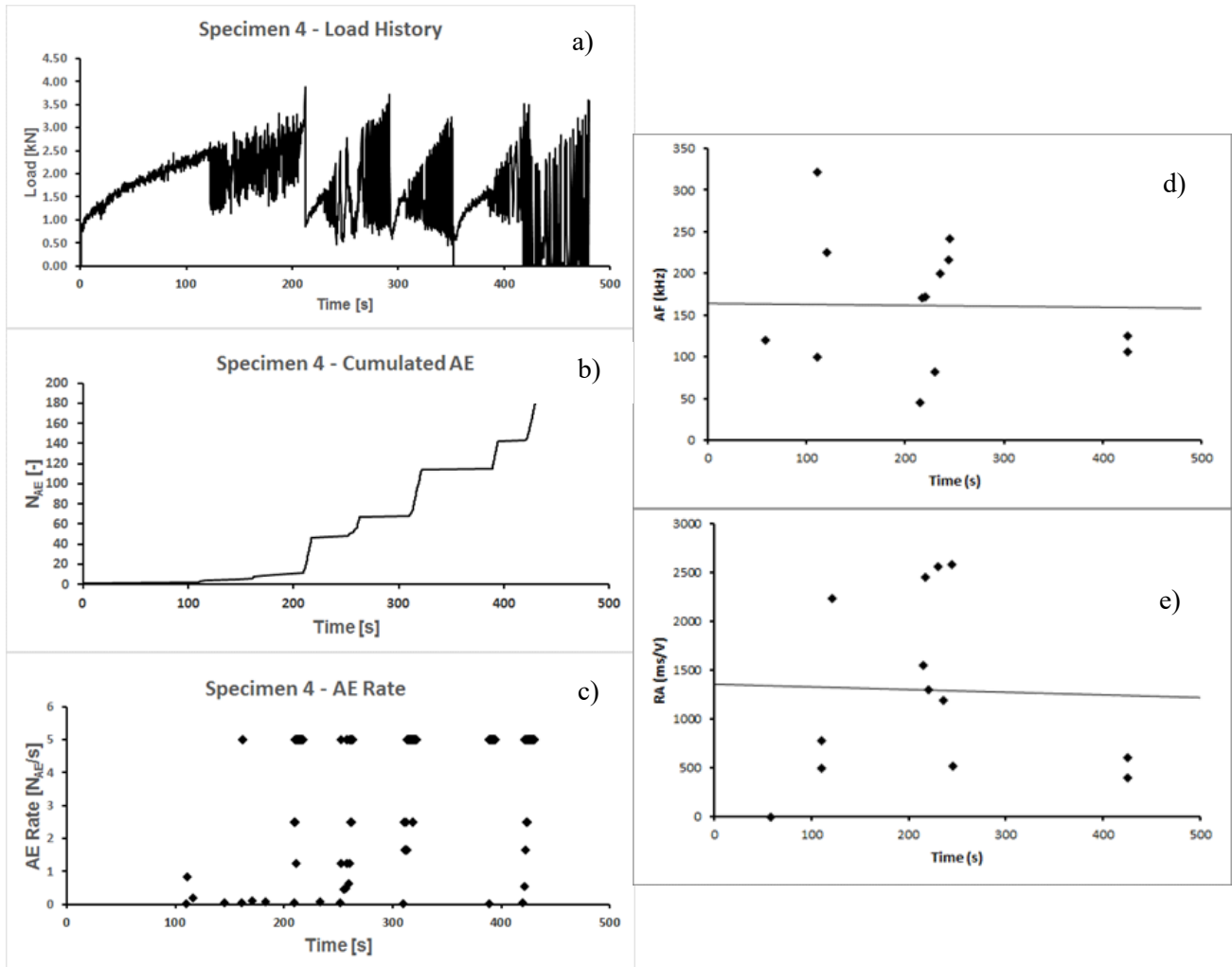


Figure 4. Diagram vs time of SM4: Load (a), Cumulated AE (b), AE rate (c), Average Frequency AF (d), Rise Angle RA (e).

4. Numerical simulation through the cohesive crack model

The most realistic method used today for the numerical simulation of mortar and stone block delamination is the cohesive crack model, also known as the Barenblatt – Dugdale - Hillerborg model for quasi-brittle materials [2]. In the present work, the crack initiation criterion is assumed as:

$$\left(\frac{\sigma_0}{f_t}\right)^2 + \left(\frac{\tau_0}{f_s}\right)^2 = 1 \quad (1)$$

where σ_0 and τ_0 are stresses evaluated along the normal and tangential to the interface directions and f_t and f_s are the related strengths. The point where equation (1) is satisfied is called the fictitious crack tip.

According to this method the cohesive stresses acting on the non-linear fracture process zone (shortened FPZ) are decreasing functions of the effective value of the displacement discontinuity w_{eff} [2, 8-12]. In this work, it was assumed:

$$w_{\text{eff}} = \sqrt{\left(\frac{w_n}{w_{nc}}\right)^2 + \left(\frac{w_t}{w_{tc}}\right)^2} \quad (2)$$

where w_n is the first component of the mutual displacement (normal to the interface) and w_t is the second one (tangential to the interface); w_{nc} and w_{tc} are the related critical values.

If $w_{\text{eff}} > 1$ no stress transfer occurs and the crack is therefore stress free, otherwise, the stresses are decreasing functions of w_{eff} that follow a pre-defined softening law. In the present work the above mentioned law is assumed as follows [2, 3, 13]:

$$\frac{\sigma}{\sigma_0} = \frac{\tau}{\tau_0} = \left[1 - \frac{1 - \exp(-\alpha \cdot w_{\text{eff}})}{1 - \exp(-\alpha)} \right] \quad (3)$$

Where $\alpha = 5$ is assumed. The point where $w_{\text{eff}} = 1$ is called real crack tip. The material outside the FPZ behaves in a linear elastic way. In a symmetric model, it is well known that the fracture process starts symmetrically, but loses this property afterwards [1, 14-16] because of the propagation of the round-off errors. In this case the numerical simulation was controlled by imposing a uniform pre-defined downward velocity to the upper edge on the rock. This choice was able to prevent the growth of the round-off errors so that, from an engineering point of view, the propagation of the two cohesive cracks occurs symmetrically. The interface strength properties were assumed as shown in Table 1-2.

Table 1. The interface strength properties

f_t (N/mm ²)	f_s (N/mm ²)	w_{nc} (mm)	w_{tc} (mm)
0.8	1.0	0,015	0,015

Table 2. Mechanical characteristics of materials

	Young's modulus (N/mm ²)	Poisson ratio
Mortar	7000	0.15
Rock	35000	0.20

The numerical analyses were executed using the ABAQUS code by applying a pre-defined downward velocity to the upper face of the stone block. The deformed finite element mesh is shown in Fig.5.

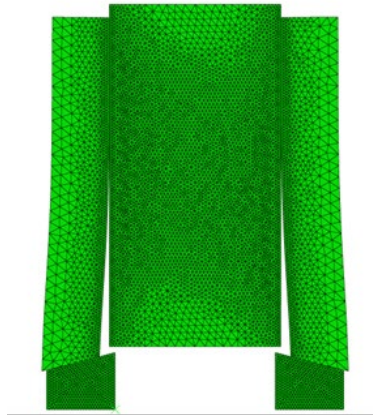


Figure 5. Finite element mesh at the maximum load. The displacements have been enlarged 100 times.

5. Experimental and numerical results

The analysis of experimental and numerical results shows four stress singularity points in the mixed specimen: two notch tips at the top, and two at the bottom (see Fig.2). For the material properties assumed, only two cohesive cracks start to propagate from the bottom side, which are the weakest points in the stress fields. A teflon sheet, inserted at the contact surface between the mortar and the steel wedges, is able to reduce the contact friction. This friction is disregarded in the numerical model that assumed the materials as homogeneous. For this reason the curve is continuous (see Fig.6). On the contrary, the properties of the rock specimen were very variable, so the experimental curve shows many discontinuities (see Fig.7). Therefore, the numerical model represents an ideal behavior, but it is not able to identify the snap-back instabilities recorded in experimental tests during the detachment progression. This process instead is well represented by the sudden increments of the AE hits [1, 2].

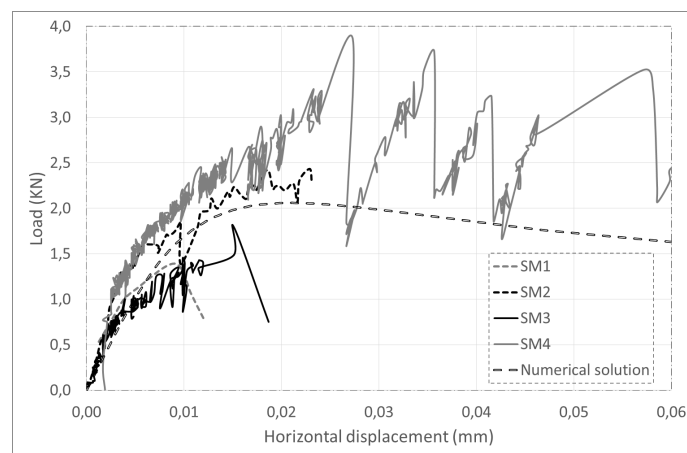


Figure 6. Load vs horizontal displacement curves of experimental test compared to numerical solution.

6. Conclusions

The AE results obtained from the compression tests on the SM4 sample prove that the AE signals are prevalent associated with the energy released by the specimen during the de-bonding of repair mortar applied in the adherence surface to masonry wall. Moreover, the variation of the AE parameters during the loading process was associated to the evolution of crack mode. The lower RA values shows more tensile fracture mode [3]. From the experimental results it was possible to identify a prevalent tensile crack behavior (Mode I) in the first phase of the delamination process. However, in the next part of the test the delamination process changes towards a slipping of the mortar (Mode II) respect to the surface of adhesion with the stone: a snap-back instabilities were recorded corresponding to a prevalent shear crack mode in the adherence surface. Finally, no prevalent fracture mode was recorded before the collapses. The non-linear phenomena at the adherence surface between mortar and stone during the detachment process were theoretically analyzed by means of the cohesive crack model [1].

7. References

- [1] Grazzini A, Lacidogna G, Valente S, et al (2018) Delamination of plasters applied to historical masonry walls: analysis by acoustic emission technique and numerical model. *IOP Conference Series: Materials Science and Engineering* 372:1-8. doi: 10.1088/1757-899X/372/1/012022.
- [2] Bocca P, Valente S, Grazzini A, et al (2014) Experimental and numerical analysis of delamination repair plaster applied to historical masonry building. *Journal of Civil Engineering and Architecture* 8:47:55. doi: 10.17265/1934-7359/2014.01.006.
- [3] Bocca P, Valente S, Grazzini A, et al (2014) Detachment analysis of dehumidified repair mortars applied to historical masonry walls. *International Journal of Architectural Heritage* 8:336–348. doi: 10.1080/15583058.2013.826304.
- [4] Bocca P, Grazzini A, (2013) Mechanical properties and freeze-thawing durability of strengthening mortars. *Journal of Materials in Civil Engineering* 25:274-280.
- [5] Carpinteri A, Grazzini A, Lacidogna G, et al (2014) Durability evaluation of reinforced masonry by fatigue tests and acoustic emission technique. *STRUCTURAL CONTROL & HEALTH MONITORING* 21:950-961. doi: 10.1002/stc.1623.
- [6] Carpinteri A, Lacidogna G, Accornero F, et al (2013) Influence of damage in the Acoustic Emission parameters. *Cement and Concrete Composites*, 44:9-16
- [7] Carpinteri A, Accornero F, (2017) Multiple snap-back instabilities in progressive microcracking coalescence, *Engineering Fracture Mechanics*, DOI: 10.1016/j.engfracmech.2017.11.034.
- [8] Barpi F, Valente S, (2010) The cohesive frictional crack model applied to the analysis of the dam-foundation joint, *Engineering Fracture Mechanics* 77:2182-2191.
- [9] Barpi F, Valente S, (2002) Fuzzy parameters analysis of time-dependent fracture of concrete dam models, *International Journal of Numerical and Analytical Method in Geomechanics* 26:1005-1027.
- [10] Barpi F, Valente S, (2004) A fractional order rate approach for modeling concrete structures subjected to creep and fracture, *International Journal of Solids and Structures* 41/9-10:2607-2621.
- [11] Barpi F, Valente S, (2005) Lifetime evaluation of concrete structures under sustained post-peak loading, *Engineering Fracture Mechanics* 72: 2427-2443.
- [12] Barpi F, Valente S, (2008) Modeling water penetration at dam-foundation joint, *Engineering Fracture Mechanics* 75/3-4: 629-642;10.1016/j.engfracmech. 2007.02.008.
- [13] Cornelissen H A W, Hordijk D A, Reinhardt H W, (1986) Experimental determination of crack softening characteristics of normal and lightweight concrete, *Heron* 31:45-56.
- [14] Barpi F, Valente S, (1998) Size-effects induced bifurcation phenomena during multiple cohesive crack propagation. *International Journal of Solids and Structures* 35(16):1851–1861.
- [15] Alberto A, Antonaci P, Valente S, (2011) Damage analysis of brick-to-mortar interfaces, 11th International Conference on the Mechanical Behavior of Materials 1151-1156.
- [16] Bocca P, Grazzini A, Masera D, et al (2011) Mechanical interaction between historical brick and repair mortar: experimental and numerical tests, *Journal of Physics* 305.